

We are IntechOpen, the world's leading publisher of Open Access books Built by scientists, for scientists

6,900

Open access books available

185,000

International authors and editors

200M

Downloads

Our authors are among the

154

Countries delivered to

TOP 1%

most cited scientists

12.2%

Contributors from top 500 universities



WEB OF SCIENCE™

Selection of our books indexed in the Book Citation Index
in Web of Science™ Core Collection (BKCI)

Interested in publishing with us?
Contact book.department@intechopen.com

Numbers displayed above are based on latest data collected.
For more information visit www.intechopen.com



Experimental Investigation on the Effect of Microwave Heating on Rock Cracking and Their Mechanical Properties

Gaoming Lu and Jianjun Zhou

Abstract

Due to various advantages including high efficiency, energy-saving, and having no secondary pollution (no dust or noise), the technology of microwave-induced fracturing of hard rock has been considered as a potential method for rock fracturing and breaking. Realizing microwave-assisted mechanical rock cutting using the microwave-induced hard rock fracturing technique can prolong the mechanical life and improve the efficiency of rock-breaking operations. For example, to realize microwave-assisted TBM excavation for hard rock tunnel. At present, this technology is still in the laboratory research stage. By summarizing the research results of relevant scholars in this field, this paper generalizes the mechanism of microwave heating of rock, microwave heating system, heating characteristics, and the effect of microwave heating on rock cracking and mechanical properties. Microwave heating causes microscopic cracks on the surface of the rock and microscopic cracks inside the rock. The higher the microwave power, the longer the irradiation time, the more serious the cracks propagation. Uniaxial compressive, Brazilian tensile, and point load strengths all decreased with increasing microwave irradiation time at rates that were positively related to the power level. The conventional triaxial compressive strength of basalt samples decreased linearly with microwave irradiation time, and the higher the confining pressure, the smaller the reduction in the strength of basalt samples after microwave treatment. In addition, the elastic modulus and Poisson's ratio of basalts decreased in a quasi-linear manner with the growth of microwave irradiation time under uniaxial compression. While microwave irradiation has a slight influence on elastic modulus and Poisson's ratio under triaxial compression. The cohesion decreases with increasing microwave irradiation time and shows an approximately linear decrease over time.

Keywords: microwave heating, TBM excavation, temperature characteristics, crack propagation, mechanical properties

1. Introduction

New, and high-efficiency technology for rock breaking is required in the field of tunnel excavation, mining and mineral processing. The technology of microwave-induced fracturing of hard rock has been considered as a potential method for

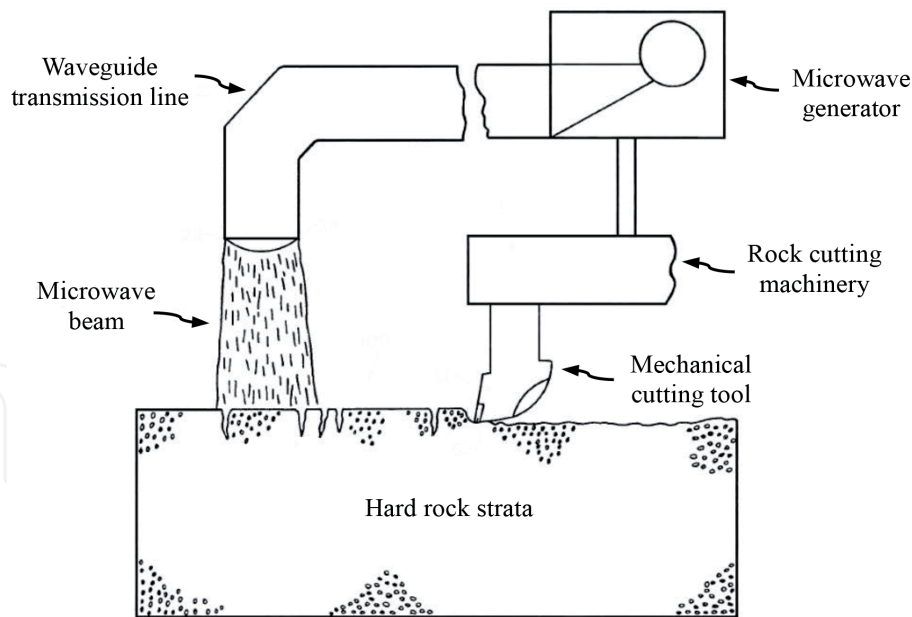


Figure 1.
Schematic diagram of microwave-assisted mechanical rock cutting [4].

rock, breaking due to various advantages including high efficiency and having no dust or noise pollution [1–3]. Realizing microwave-assisted mechanical rock cutting (**Figure 1**) using the microwave-induced hard rock fracturing technique can prolong the mechanical life and improve the efficiency of rock breaking operations [4–7]. At present, tunnel boring machines (TBMs) and shield machines have been increasingly used in tunnel excavation. The shield machine is subjected to a series of problems such as deformation of the tool apron and severe cutter wear due to the presence of boulders [8–10]. During the tunneling of hard rocks by TBMs, the disc cutter is worn and frequently changed-out, thus increasing the cost of maintenance and influencing construction progress [11–14].

The design of cutter heads of shield machines and TBMs is closely related to the properties of rocks and prevailing geological conditions [15, 16]. The mechanical strengths (uniaxial compressive strength, tensile strength, and point load strength, etc.) of rocks are important parameters influencing the service life and penetration of disc cutters on TBMs [17, 18]. Microwave treatment can significantly decrease the strength of rocks [3, 19–22], and thus can improve the penetration and life of disc cutters. Therefore, by introducing microwave heating technology into TBMs or shield machines, hard rocks or boulders can be pre-fractured through microwave irradiation. In this way, cutter wear can be reduced to increase efficiency in tunnel excavation.

Some scholars have carried out numerous experiments and numerical research into the mechanism governing the microwave-induced fracturing of rocks (or ores) and the influence of microwave treatment on the mechanical properties of rocks (or ores) [23–25]. Under the effect of microwave treatment, new intergranular and transgranular fractures are generated in rocks [26] to lead to the reduction of work index [27, 28] and strengths (including uniaxial strength, Brazilian splitting strength, and point load strength) of rocks [2, 29, 30]. More seriously, rocks are cracked and crushed or molten to cause rocks (or ores) to lose all of their bearing capacity [29, 31]. Hassani et al. [3, 6, 32] and Nekoovaght et al. [33, 34] studied the influence of microwave power and irradiation time on the strength of different kinds of rocks by using a frequency of 2450 MHz multi-mode cavity. In addition, they also studied the influence of the distance between the microwave antenna and the rock on the heating characteristics by experiments and numerical comparison.

Peinsitt et al. [35] explored the effects of microwave irradiation on the strength, acoustic velocity, and heating effect of three types of dry and saturated rocks using a 2450 MHz multi-mode cavity. By using an open-ended waveguide set-up at a frequency of 2,450 MHz, Hartlieb et al. [36–38] explored the failure mechanism and thermal physical characteristics of different types of rocks. Lu et al. [29, 39, 40] studied the mechanism, temperature distribution, and crack propagation of microwave-heated rocks using a multi-mode resonator.

At present, the technology of microwave-induced fracturing of hard rock is still in the laboratory research stage. By summarizing the research results of relevant scholars in this field, this work generalizes the mechanism of microwave heating of rock, microwave heating system, heating characteristics, and the effect of microwave heating on rock cracking and mechanical properties.

2. Principle of microwave heating rocks

When a dielectric material is subjected to an alternating current, it absorbs electrical energy, which is dissipated in the form of heat (the dielectric loss). The dielectric constant of the material consists of the real part and the imaginary part, as shown below

$$\varepsilon = \varepsilon' - j\varepsilon'' \quad (1)$$

where the real part (ε') is known as the dielectric constant. The imaginary part (ε'') is known as the loss factor [41].

The loss tangent ($\tan \delta$) is the ratio of the imaginary part (ε'') to the real part (ε'), i.e.

$$\tan \delta = \frac{\varepsilon''}{\varepsilon'} \quad (2)$$

It measures the ability of the dielectric to store energy and convert it into heat.

The microwave absorption capacity of electrolyte material is related to its dielectric properties. The microwave heating mechanism of minerals and rocks in the electromagnetic field is usually expressed by the power density, which can be expressed by the following Equation

$$P = 2\pi\varepsilon_0\varepsilon''E^2f \quad (3)$$

where P is the loss power density deposited within the sample; E is the electric field and f is the microwave frequency; ε_0 is the dielectric constant of free space (8.85×10^{-12} F/m) [42].

The temperature of the dielectric material increases when it absorbs microwave energy [41]. According to the laws of thermodynamics the amount of energy required to increase the temperature of a material to a given amount is calculated by the following equations

$$Q = Cm\Delta T \quad (4)$$

$$P = \rho C \frac{\Delta T}{\Delta t} \quad (5)$$

where Q is the energy absorbed by the material; C is the specific heat capacity; m is the mass; ΔT is the temperature increase after absorbing energy; Δt is the time difference.

By combining Eqs. (3) and (5), the rate of heating may be given by

$$\frac{\Delta T}{\Delta t} = \frac{2\pi\epsilon_0\epsilon''E^2f}{\rho C} \quad (6)$$

An increase in material temperature causes the volume of the material to increase

$$V(T) = V_0 (1 + \alpha \Delta T) \quad (7)$$

where, V_0 is the volume at some reference temperature, and α is the coefficient of thermal expansion of the medium [43].

After being irradiated by microwaves, rocks absorb electromagnetic energy that is transformed into thermal energy, causing the temperature rising of rocks. After microwave irradiation, the temperature of the rocks is not uniform, resulting in uneven thermal expansion in the rocks. Different minerals within rocks have different dielectric properties, leading to different rocks have different microwave absorption capacities. Different minerals also have different thermal expansion coefficients, so the thermal expansion property is different after heating. Therefore, due to the different microwave sensitivity and thermal expansibility of different types of rocks, different types of rocks show different heating characteristics and fracturing effects.

3. Microwave heating system for rock

The microwave heating equipment includes a power supply, a magnetron, an isolator, a coupler, an impedance tuner, a rectangular waveguide, a microwave applicator, and a shielded cavity (**Figure 2**). The power supply is used to convert alternating-current into direct-current to thus create conditions for the operation

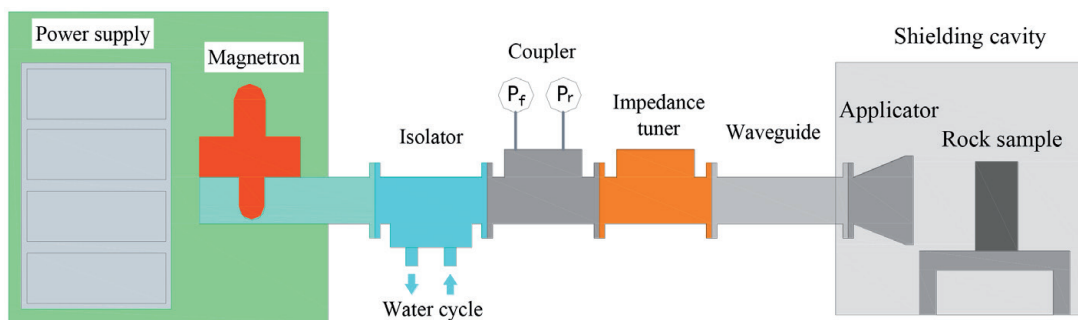


Figure 2.
Schematic view of the microwave heating system.

of the magnetron. The magnetron converts direct-current electrical energy into microwave energy, thus providing continuous microwave power. The isolator is used for the unidirectional circular transmission of microwave energy. The function of the water cycle is to absorb the reflected microwave energy, thus protecting the magnetron from damage. The microwave applicator is used to emit microwave energy to the surface of rocks, where it is used to heat and crack rocks. The impedance tuner is used for impedance matching. Compared with the microwave source with a frequency of 915 MHz, the microwave source with a frequency of 2450 MHz has higher heating efficiency and smaller volume, which is conducive to the combination with the mechanical rock-breaking device. During testing, a metal net is used as shielding to avoid microwave interference with signal transmission to/from the other apparatuses.

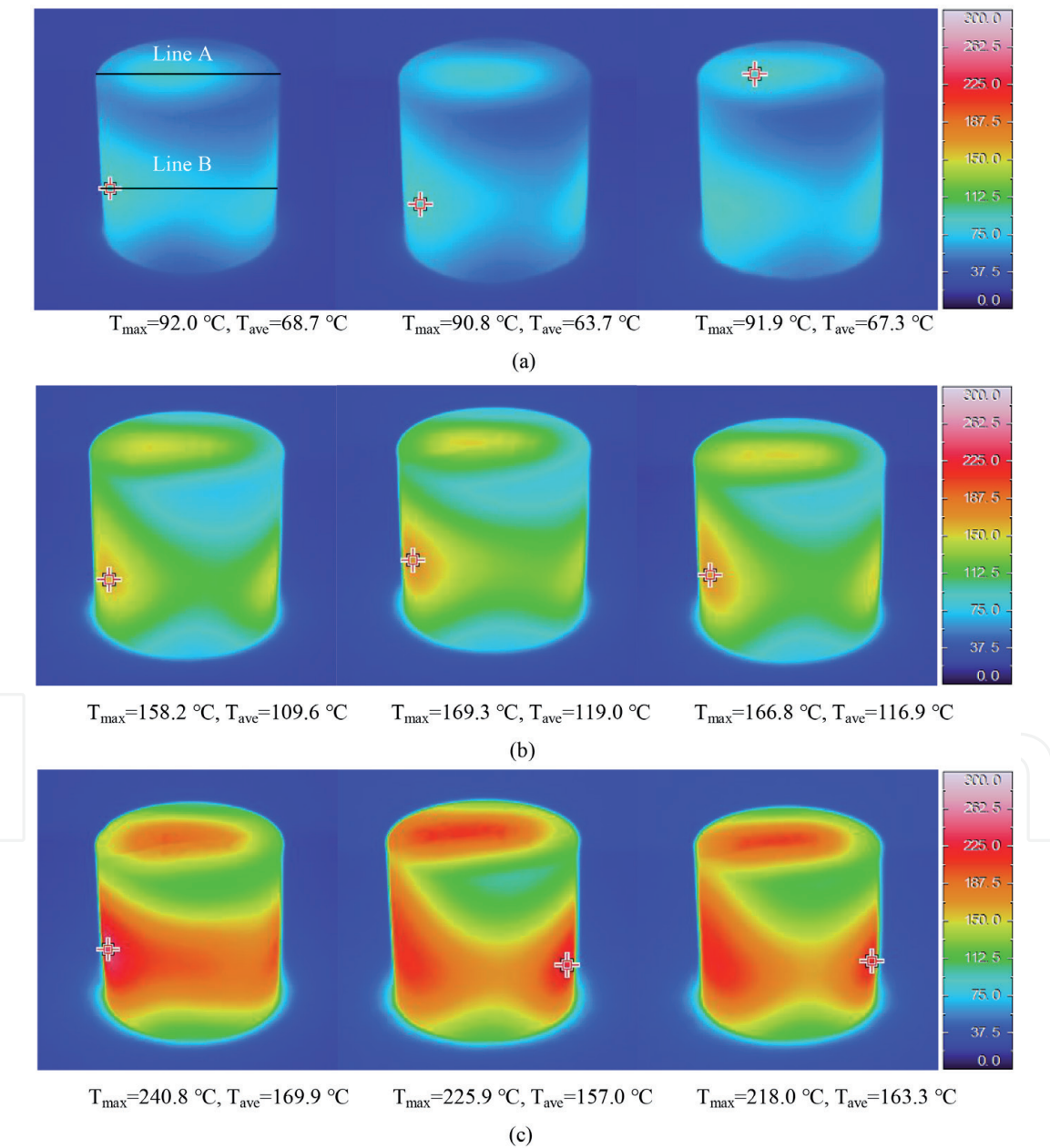


Figure 3. Temperature distribution on the surface of samples measured by infrared camera (ambient temperature at 13.5°C) [44]. $T_{max} = 92.0^{\circ}\text{C}$, $T_{ave} = 68.7^{\circ}\text{C}$ $T_{max} = 90.8^{\circ}\text{C}$, $T_{ave} = 63.7^{\circ}\text{C}$ $T_{max} = 91.9^{\circ}\text{C}$, $T_{ave} = 67.3^{\circ}\text{C}$ (a) 5 kW, 10 s. $T_{max} = 158.2^{\circ}\text{C}$, $T_{ave} = 109.6^{\circ}\text{C}$ $T_{max} = 169.3^{\circ}\text{C}$, $T_{ave} = 119.0^{\circ}\text{C}$ $T_{max} = 166.8^{\circ}\text{C}$, $T_{ave} = 116.9^{\circ}\text{C}$ (b) 5 kW, 20 s. $T_{max} = 240.8^{\circ}\text{C}$, $T_{ave} = 169.9^{\circ}\text{C}$ $T_{max} = 225.9^{\circ}\text{C}$, $T_{ave} = 157.0^{\circ}\text{C}$ $T_{max} = 218.0^{\circ}\text{C}$, $T_{ave} = 163.3^{\circ}\text{C}$. (c) 5 kW, 30 s.

4. Temperature characteristics

Figures 3 and 4 show the temperature distributions on the surface of samples and along their straight lines [44]. As is seen, the surface temperature of samples was non-uniformly distributed, i.e. the longer the irradiation time, the more non-uniform the temperature distribution. A local high-temperature region occurred on the surface of the cylindrical samples. The temperature inside the samples was higher than that on the surface of the samples, and the maximum temperature occurred near the center of the samples. There were two high-temperature zones at the left and right sides of the lower part of the cylinder sample surface. The non-uniformity of temperature distribution led to the non-uniformity of thermal expansion within the samples, which will promote the cracking and fracturing of samples. The influence of irradiation time on the surface temperature of the basalt samples is shown in **Figure 5**. As is seen, after microwave irradiation for 10 s, 20 s, and 30 s, the maximum temperatures were 91.6°C, 164.8°C, and 228.2°C at a microwave power of 5 kW while the average temperatures were 66.6°C, 115.2°C, and

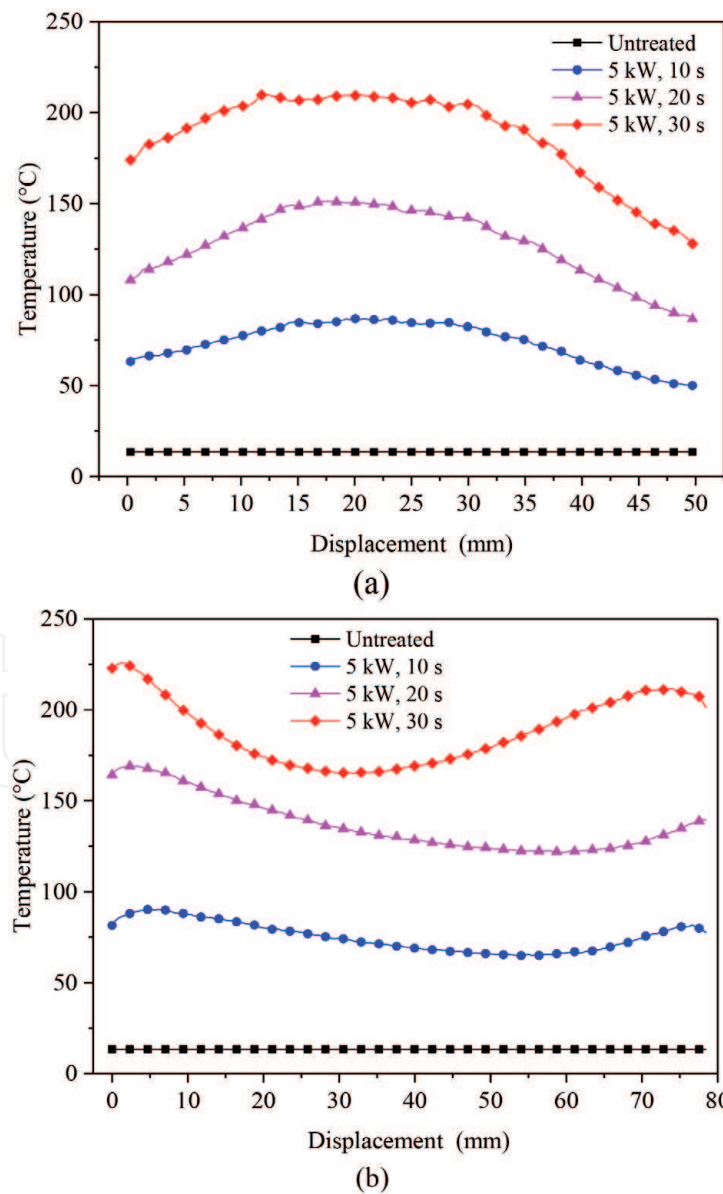


Figure 4. Temperature distributions along straight lines of samples passing the point with the highest temperature [44]. (a) the upper surface (line a). (b) Cylindrical surface (line B).

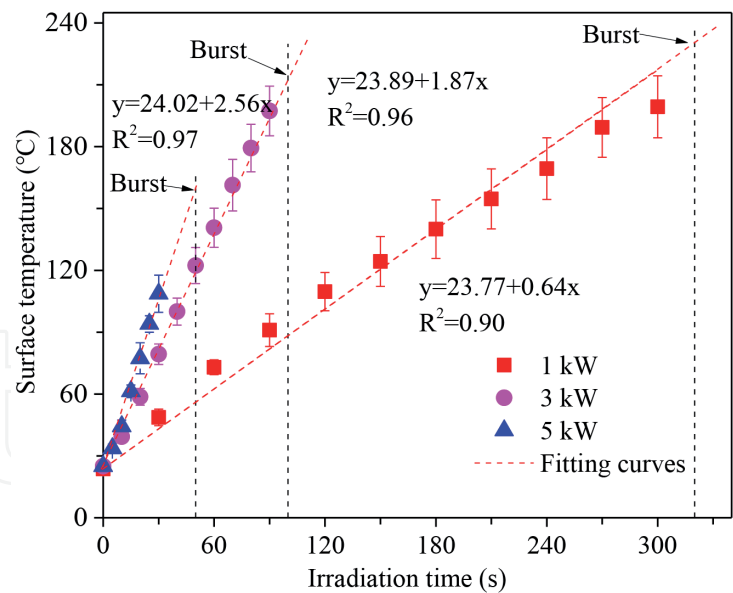


Figure 5.
Surface temperature vs. irradiation time of $\Phi 50 \times 100$ mm cylindrical basalt specimens [29].

163.4°C, respectively. When the microwave power is constant, the maximum and average temperature on the surface of the samples both linearly increased with the irradiation time (**Figure 5**). The longer the microwave irradiation time, the higher the surface temperature of the samples.

The surface temperatures of the cylindrical basalt samples increased with the increase of irradiation time at each of the three microwave powers (**Figure 5**) [29]. The surface temperature of the sample increased linearly with the microwave irradiation time, and the heating rate increased with the growth of microwave power. Samples burst at approximately 230°C and 320 s at 1 kW, 210°C and 100 s at 3 kW, and 160°C and 50 s at 5 kW. The broken pieces began to melt with increasing the irradiation time. The higher the microwave power input, the faster the rate of heating, and the shorter the time needed for the sample to bursting.

5. Effect of microwave heating on crack propagation of rock samples

5.1 Microscopic crack propagation

Under the conditions of 5 kW power and different microwave irradiation times, the crack propagation on the surface of the 50 mm cubic samples was observed with an ultra-depth field microscope, as shown in **Figure 6**. Compared with the untreated cubic samples, more intragranular and intergranular cracks were observed around and along the olivine granules. With the increase of microwave irradiation time, cracks became wider and more pronounced. Relative to untreated samples, intergranular and intragranular microscopic cracks occurred within cylindrical samples after microwave treatment for 60 s at 3 kW.

After microwave irradiation, more intergranular and transgranular cracks occurred within the basalt samples. In particular, the intergranular cracks mainly occurred between plagioclase and olivine, while the intragranular cracks mainly occurred within the olivine grains. With the increase of intergranular cracks and intragranular cracks, macroscopic cracks mainly occurred across the area where olivine and enstatite grains gathered. This is because enstatite provides the energy needed for the thermal expansion of olivine [29, 39].

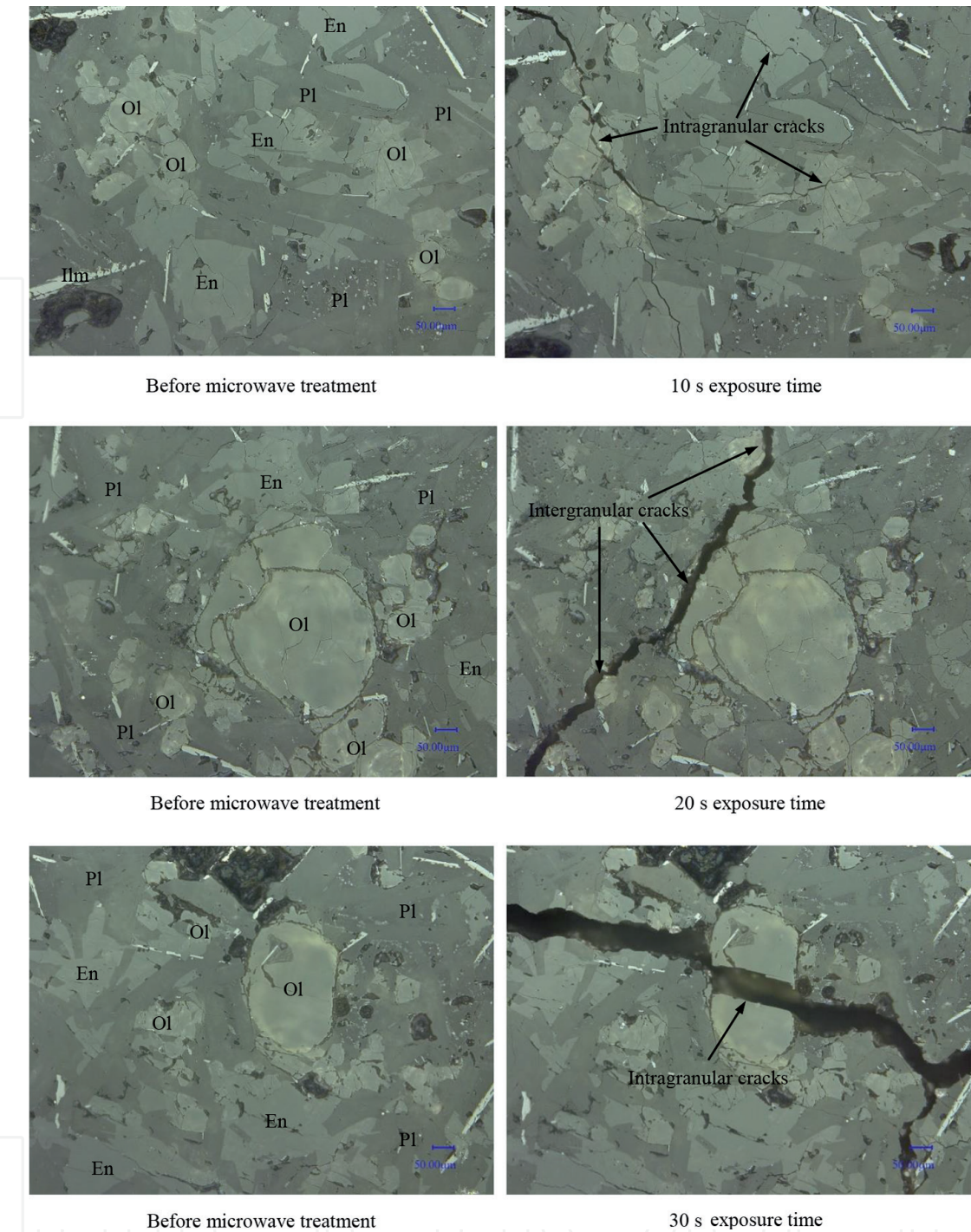


Figure 6. Microscopic crack propagation on the surface of 50 mm cubic basalt specimens viewed under an ultra-depth of field microscope at 300× magnification before (left) and after (right) microwave treatment at 5 kW power and three exposure times [39].

5.2 Macroscopic crack propagation

The typical pattern of macroscopic crack propagation on the surface of the cylindrical samples is shown in **Figure 7** [29]. It can be seen that the macroscopic cracks of the microwave-treated cylindrical samples propagated on the two end surfaces and the cylindrical curved surface of the cylindrical samples. The main crack on the cylinder was approximately parallel to the axis of the cylinder and connected to the crack on the end surfaces. After a long time of microwave irradiation, about three cracks propagated on the end surfaces of the sample, converging to a point near the center of the circle. The sample with low microwave power or short irradiation time had less crack propagation. With the increase of microwave irradiation time or microwave

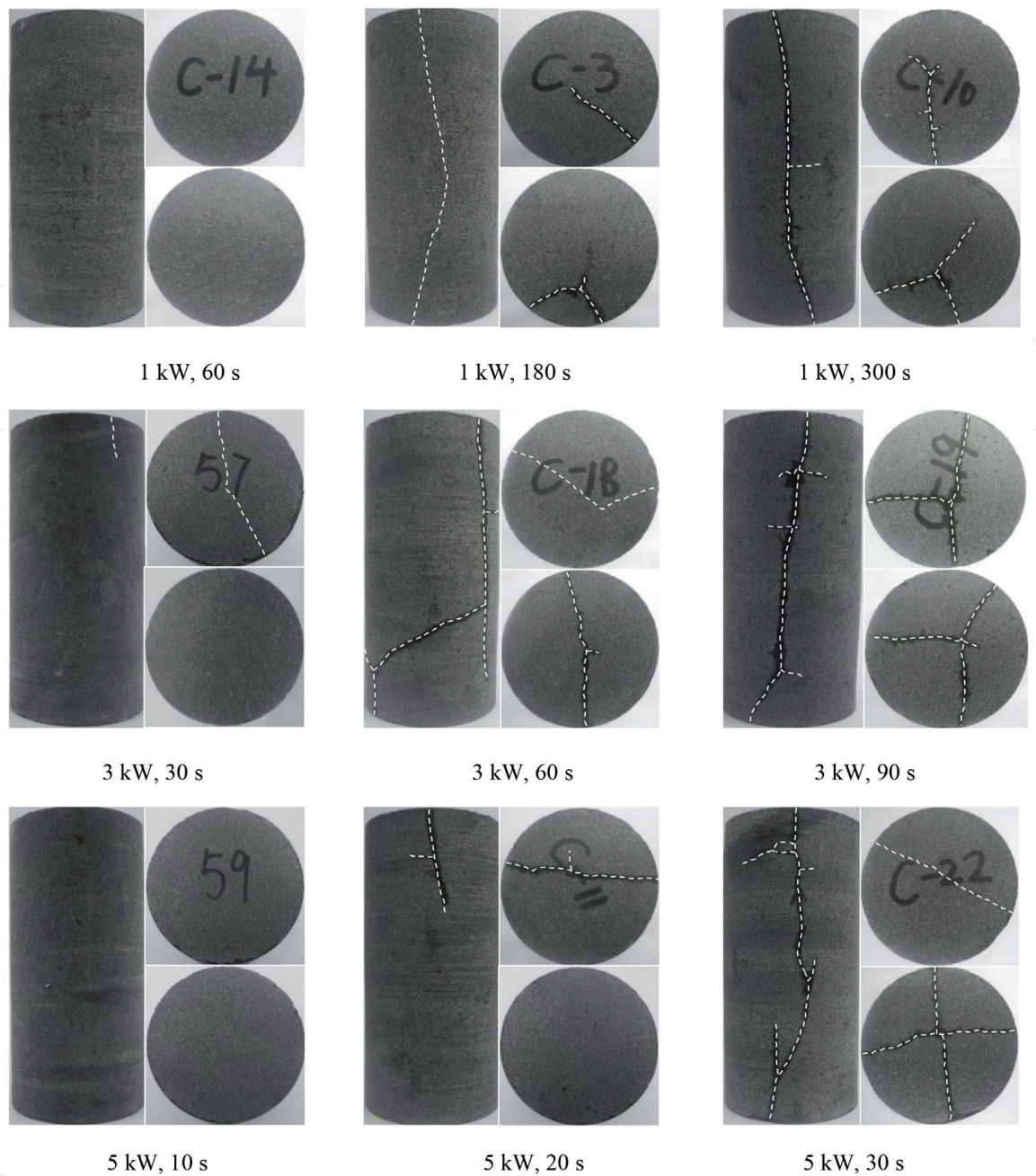


Figure 7.
Typical pattern of macroscopic crack propagation on the surface of cylindrical specimens induced by microwave irradiation at three power levels and seven exposure times [29].

power, the length and number of cracks increased gradually. Microwave power and irradiation time are important parameters affecting crack generation. The higher the microwave power, the shorter the time needed to generate cracks of the same degree.

6. Effect of microwave heating on mechanical properties of rock

6.1 Mechanical strength

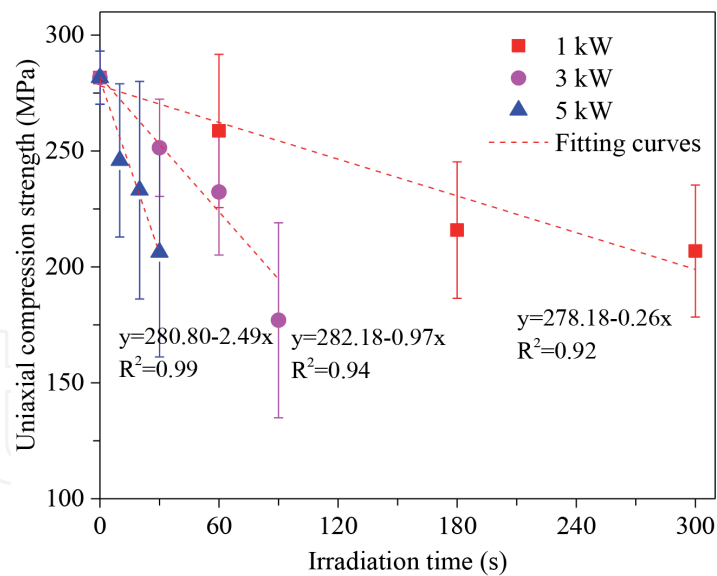
After microwave irradiation, the uniaxial compression strength decreases with the increase of microwave irradiation time at three microwave powers (1 kW, 3 kW, and 5 kW). The uniaxial compression strength decreases in an approximately linear manner with increasing microwave irradiation time. The greater the applied microwave power, the faster the decrease rate of uniaxial

compression strength [29]. Pyroxene is a highly microwave-absorbing mineral and has strong heating ability after microwave irradiation. Olivine is a strong thermal expansion mineral, which can produce strong thermal expansion under high temperatures. As a result, transgranular cracks mainly occurred in olivine particles, and intergranular cracks mainly occurred between olivines and plagioclases. With the increase of microwave irradiation time, the microcracks slip and connect, forming weak planes in the rocks. Compared with the rocks not irradiated by microwave, the strength of the rocks decreased to different extents. The longer the microwave irradiation time or the higher the microwave power, the more developed the weak surface and the greater the strength reduction.

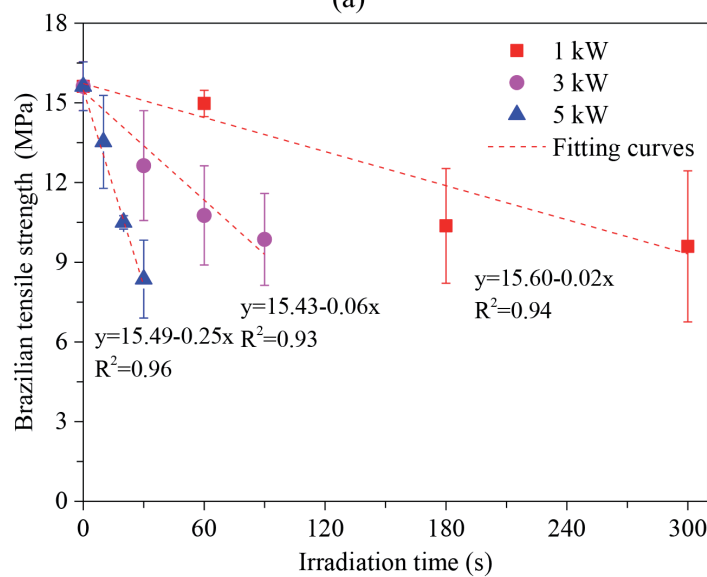
Figure 8 shows the relationships between the mechanical strength of a basalt and microwave irradiation time for different microwave power levels. As illustrated in **Figure 8(a-c)**, the uniaxial compression strength (a), the Brazilian tensile strength (b), and the point load strength (c) decreased with irradiation time at each power level. Overall, the magnitude of the reductions was least for uniaxial compression strength, and most for point load strength. According to the slope of the fitting curves, the higher the microwave power, the faster the rock strength decreased. For example, the Brazilian tensile strength was reduced by approximately 39% at 1 kW power after 300 s irradiation, 37% at 3 kW power after 90 s irradiation, and 46% at 5 kW power after 30 s irradiation. Similarly, the uniaxial compression strength was reduced by less than 11% at 3 kW power and by 27% at 5 kW power after 30 s irradiation. Under the three microwave powers, Uniaxial compressive, Brazilian tensile, and point load strength were reduced by up to 37%, 46% and 62% respectively. Microwave power and irradiation time are important parameters affecting basalt strength, and the reduction of strength has an approximately linear relationship with the irradiation time at each power level.

At the applied power of 5 kW, the relationship between conventional triaxial compressive strength of basalts and microwave irradiation time is shown in **Figure 9** [45]. Under four confining pressures ($\sigma_3 = 0$ MPa, 10 MPa, 30 MPa, and 50 MPa), the conventional triaxial compressive strength reduces at different rates with increasing microwave irradiation time. At 30 s irradiation, the conventional triaxial compressive strength reduces by 27%, 7%, 2%, and 1% under the four confining pressures, respectively. It is worth noting that, with the increase in confining pressure, the conventional triaxial compressive strength of the basalts gradually reduces (The test value has a certain discreteness, and the overall effect is reduced.). Confining pressure closes part of the cracks induced by microwave irradiation and increases the frictional forces that prevent slippage of microcracks. Therefore, confining pressure inhibits the reduction of conventional triaxial compressive strength and discreteness. The discreteness of conventional triaxial compressive strength is mainly caused by the heterogeneity of microcracks, while the confining pressure leads to the closure of microcracks in the samples and reduction of microcracks that produce slippage. Therefore, the confining pressure can decrease the discreteness of conventional triaxial compressive strength. Geological factors such as in situ stress should be considered when microwave-induced fracturing is used in underground geotechnical engineering [45].

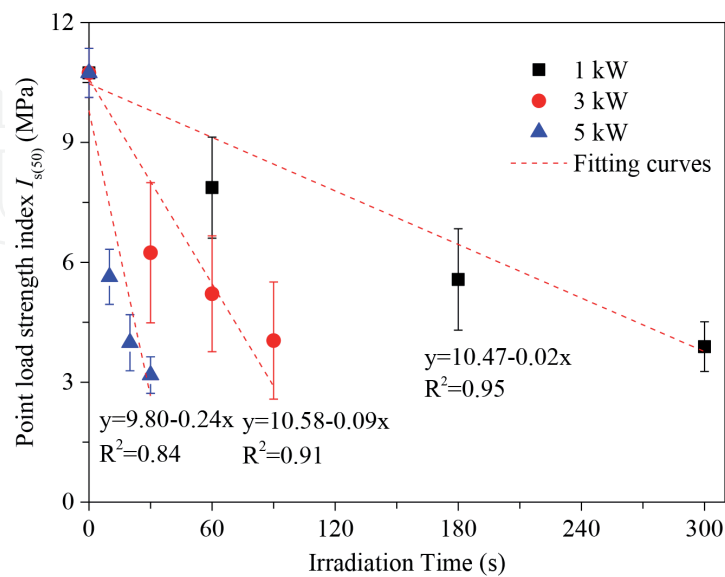
Due to rocks are heterogeneous materials, differences between samples can lead to the discreteness of test results. The existence of microwave sensitive minerals and strong thermal expansion minerals results in the random distribution of microcracks in different directions within the rocks after microwave irradiation. After microwave irradiation, microcracks occurred within the rock, which can further increase the dispersion of the test results. The higher the microwave power



(a)



(b)



(c)

Figure 8.
Relationships between mechanical strength of basalt and microwave irradiation time for three power levels: (a) uniaxial compressive strength, (b) Brazilian tensile strength, and (c) point load strength [29].

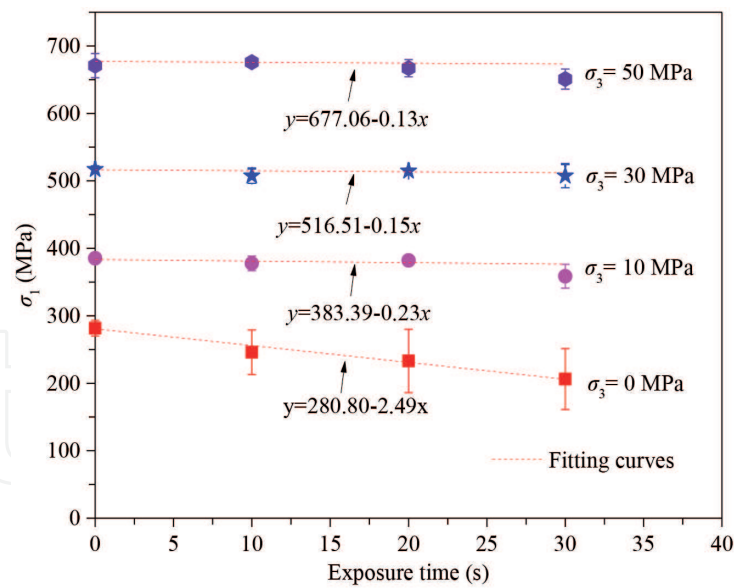


Figure 9.
Reductions in compression strength of basalts under different confining pressures [45].

and the longer the irradiation time, the more discreteness the test results will be. When significant crack propagation or weak surface occurs in the rock, the bearing capacity of the rock will be significantly reduced, leading to the decrease of the rock strength. It is revealed that the confining pressure inhibits discreteness of basalt strength and the strength differences induced by microcracking gradually decrease with increasing confining pressure.

6.2 Elastic modulus and Poisson’s ratio

The average elastic modulus and Poisson’s ratio are calculated by linear fitting of the stress–strain curve. The elastic modulus and Poisson’s ratio are calculated by linear fitting of the stress–strain curve, and the calculation results are shown in **Figures 10** and **11**. The basalt has a compact structure and the average elastic modulus before microwave irradiation is 97 GPa. After microwave irradiation,

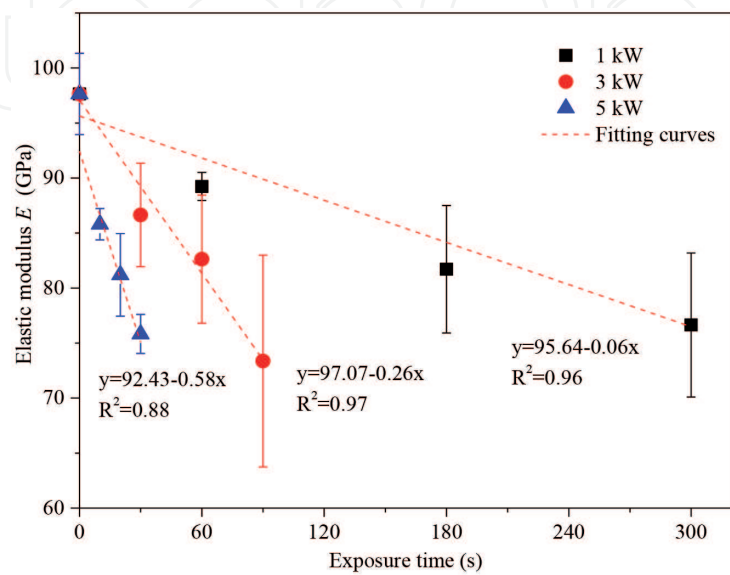


Figure 10.
Relationships between elastic modulus of basalts and microwave exposure time under uniaxial compression [45].

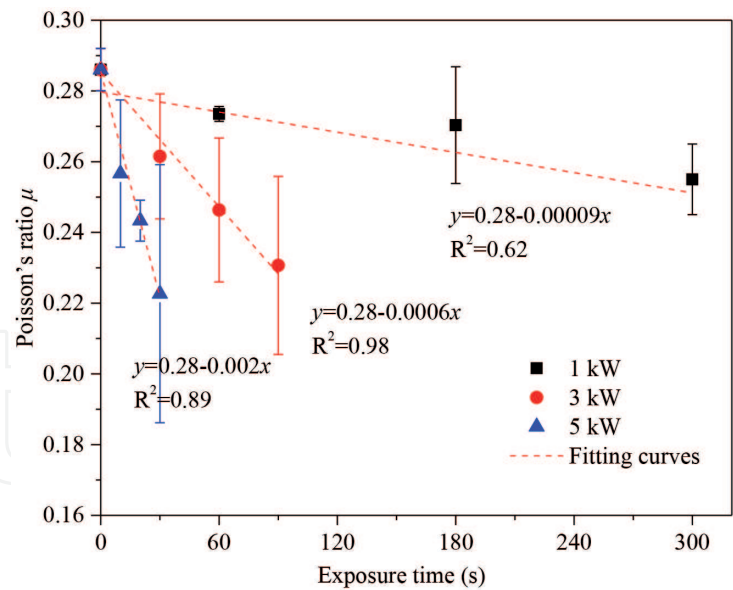


Figure 11.
Relationships between Poisson's ratio of basalts and microwave exposure time under uniaxial compression [45].

the elastic modulus and Poisson's ratio both decrease at three power levels (1 kW, 3 kW, and 5 kW). The decrease rate of elastic modulus is greater than Poisson's ratio at the three power levels, and elastic moduli are decreased by 22%, 25%, and 22%, while the Poisson's ratios decrease by 11%, 19%, and 22%, respectively. The elastic modulus and Poisson's ratio decrease linearly with the microwave irradiation time. According to the slopes of the fitting curves, it is known that the higher the microwave power, the greater the degree of reduction of elastic modulus and Poisson's ratio.

After microwave treatment, the decrease of elastic modulus indicates that microwave irradiation can reduce the stiffness of rocks, that is to say, it can reduce the bearing capacity of rocks. As is known, in the compression test, the elastic deformation of rocks is mainly determined by the skeleton of mineral particles. Transgranular fracture and intergranular cracks can be induced in and between mineral particles by microwave treatment. With the increase and penetration of these microcracks, new cracks will be formed. Therefore, microwave irradiation changes the skeleton structure of mineral particles in the rocks and weakens the resistance of the rocks to elastic deformation.

6.3 Cohesion and internal friction angle

In the field of rock mechanics, cohesion refers to the attraction between molecules on the surface of adjacent mineral particles. After microwave treatment, the peak strength of the samples at different irradiation times presented monotonically increasing relation with confining pressure, which was in accordance with the Coulomb strength criterion. The cohesion c and internal friction angle ϕ of basalt samples were calculated according to the Coulomb strength criterion (**Table 1** and **Figure 12**). After microwave treatment, the cohesion of the samples decreased linearly with the increase of microwave irradiation time. When the microwave power is 5 kW and the microwave irradiation time is 10 s, 20 s, and 30 s, the cohesion decreases by 14%, 13%, and 25% respectively. After microwave treatment, transgranular and intergranular cracks were generated within and between mineral particles, which reduced the cementation between mineral particles and thus reduced the overall cohesion. While the internal friction angle increases slightly after microwave treatment.

Exposure time (s)	σ_3 (MPa)	σ_1 (MPa)	c (MPa)	φ (°)
0	0	281.7	54.26	50.03
	10	385.33		
	30	518		
	50	671		
10	0	245.9	46.41	51.59
	10	377.67		
	30	507.33		
	50	676.33		
20	0	233.1	47.09	51.63
	10	382		
	30	514.67		
	50	667		
30	0	206.3	40.93	52.18
	10	358.67		
	30	507.33		
	50	650.67		

Table 1.
Conventional triaxial compressive strength test results of basalt samples at different exposure times [45].

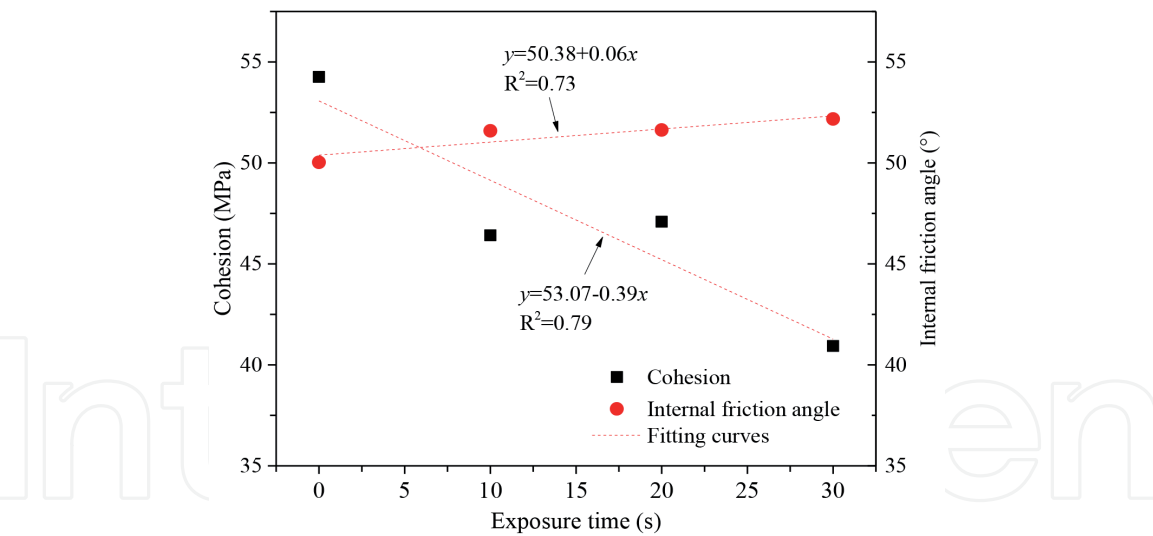


Figure 12.
Relationships between cohesion and internal friction angle of the basalts with microwave exposure time [45].

7. Summary and conclusions

Microwave power level had a significant positive relationship with basalt heating rate: the higher the applied power, the faster the basalt temperature rises. The surface temperature of the sample is not uniformly distributed, which is conducive to the generation of cracks. The higher the microwave power, the more serious the crack propagation. As the number of fractures increased, visible cracks were generated, leading to significant strength reduction. The Uniaxial compressive, Brazilian tensile, and point load strength all decreased after irradiation at each of the three

power levels; the higher the power level, the faster the strength decreased. Under the three microwave powers, Uniaxial compressive, Brazilian tensile, and point load strength were reduced by up to 37%, 46%, and 62% respectively. The conventional triaxial compressive strength decreased linearly with microwave irradiation time, and the higher the confining pressure, the smaller the reduction in the strength of basalt samples after microwave treatment. At 30 s irradiation, the conventional triaxial compressive strength reduces by 27%, 7%, 2%, and 1% under the four confining pressures ($\sigma_3 = 0$ MPa, 10 MPa, 30 MPa, and 50 MPa), respectively.

The elastic modulus and Poisson's ratio of basalts also decreased in a quasi-linear manner with elapsed microwave irradiation time. At the three applied powers, the decrease rate in elastic modulus always exceeds that of the Poisson's ratio, and elastic moduli are decreased by 22%, 25%, and 22%, while the Poisson's ratios decrease by 11%, 19%, and 22%, respectively. The confining pressure results in the closure of the microcracks caused by microwave irradiation, so the influence of microwave treatment on strength and deformation is reduced, leading to a decrease in the influence on the elastic constants. The cohesion decreases with the increase of microwave irradiation time and presents an approximate linear decreasing relationship. At microwave power of 5 kW and irradiation times of 10 s, 20 s, and 30 s, the cohesion is reduced by 14%, 13%, and 25%, respectively. In the basalt samples, new microcracks in various directions generated by microwave irradiation can increase the discreteness of test results, while the discreteness of test results caused by microcracks gradually reduces with increasing confining pressure.

Uniaxial compressive, Brazilian tensile, and point load strength are important parameters that affect the service life and the penetration of mechanical rock-breaking tools. The reduction of rock strength can increase the service life and the penetration of mechanical rock-breaking tools. Microwave irradiation weakens the mechanical properties of rock, which effectively reduces the resistance of the rock to the mechanical rock-breaking tool, which can reduce the wear of the mechanical rock-breaking tool and improve the rock-breaking efficiency. Microwave-assisted rock-breaking has significant potential application to in-situ mining, tunneling, rock breakage, and comminution.

Acknowledgements

Financial support for this work by the National Natural Science Foundation of China (No: 42002281), by the Natural Science Foundation of Henan Province (No: 202300410002, 212300410325), by the Science and Technology Research and Development Plan of China Railway Group Limited (No: 2020-Zhongda-06) and the Science and Technology Innovation Plan of China Railway Tunnel Group (No: Suiyanhe 2020-11) are greatly appreciated.

IntechOpen

Author details

Gaoming Lu^{1,2*} and Jianjun Zhou^{1,2}

1 State Key Laboratory of Shield Machine and Boring Technology, Zhengzhou, China

2 China Railway Tunnel Group Co., Ltd, Guangzhou, China

*Address all correspondence to: gaoming_lu@foxmail.com

IntechOpen

© 2021 The Author(s). Licensee IntechOpen. This chapter is distributed under the terms of the Creative Commons Attribution License (<http://creativecommons.org/licenses/by/3.0>), which permits unrestricted use, distribution, and reproduction in any medium, provided the original work is properly cited. 

References

- [1] Lu GM, Feng XT, Li YH, Zhang XW. The Microwave-Induced Fracturing of Hard Rock[J]. *Rock Mechanics and Rock Engineering*, 2019, 52(9): 3017-3032.
- [2] Lu GM. Experimental study on the microwave fracturing of hard rock[D]. Northeastern University, 2018.
- [3] Hassani F, Nekoovaght PM, Gharib N. The influence of microwave irradiation on rocks for microwave-assisted underground excavation[J]. *Journal of Rock Mechanics and Geotechnical Engineering*, 2016, 8(1): 1-15.
- [4] Lindroth DP, Morrell RJ, Blair JR. Microwave assisted hard rock cutting: US5003144[P]. 1991.
- [5] Feng XT, Lu GM, Li YH, Zhang XW. Cutter head for microwave presplitting type hard-rock tunnel boring machine: US10428654B2[P]. 2019.
- [6] Hassani F, Nekoovaght P. The development of microwave assisted machineries to break hard rocks[C]// *Proceedings of the 28th International Symposium on Automation and Robotics in Construction (ISARC)*, Seoul, 2011: 678-684.
- [7] Ouellet J, Radziszewski P, Raghavan V, Hemanth S. Electromagnetic energy assisted drilling system and method: US8550182B2[P]. 2019-1-1.
- [8] Nishitake S. Earth pressure balanced shield machine to cope with boulders[J]. *International Journal of Rock Mechanics and Mining Sciences & Geomechanics Abstracts*, 1989, 1(6): 552-572.
- [9] Filbà M, Salvany JM, Jubany J, Carrasco L. Tunnel boring machine collision with an ancient boulder beach during the excavation of the Barcelona city subway L10 line: A case of adverse geology and resulting engineering solutions[J]. *Engineering Geology*, 2016, 200(2): 31-46.
- [10] Li XG, Yuan DJ. Creating a working space for modifying and maintaining the cutterhead of a large-diameter slurry shield: A case study of Beijing railway tunnel construction[J]. *Tunnelling and Underground Space Technology*, 2018, 72(2): 73-83.
- [11] Jain P, Naithani AK, Singh TN. Performance characteristics of tunnel boring machine in basalt and pyroclastic rocks of Deccan traps—A case study[J]. *Journal of Rock Mechanics and Geotechnical Engineering*, 2014(1): 36-47.
- [12] Entacher M, Lorenz S, Galler R. Tunnel boring machine performance prediction with scaled rock cutting tests[J]. *International Journal of Rock Mechanics and Mining Sciences*, 2014, 70(9): 450-459.
- [13] Xia YM, Zhang K, Liu JS. Design optimization of TBM disc cutters for different geological conditions[J]. *World Journal of Engineering and Technology*, 2015(4): 218-231.
- [14] Rostami J. Performance prediction of hard rock Tunnel Boring Machines (TBMs) in difficult ground[J]. *Tunnelling and Underground Space Technology*, 2016, 57: 173-182.
- [15] Xia YM, Ouyang T, Zhang XM, Luo DZ. Mechanical model of breaking rock and force characteristic of disc cutter[J]. *Journal of Central South University*, 2012, 19(7): 1846-1858.
- [16] Deliormanlı AH. Cerchar abrasivity index (CAI) and its relation to strength and abrasion test methods for marble stones[J]. *Construction and Building Materials*, 2012, 30: 16-21.

- [17] Wijk G. A model of tunnel boring machine performance[J]. *Geotechnical & Geological Engineering*, 1992, 10(1): 19-40.
- [18] Boniface A. Tunnel boring machine performance in basalts of the Lesotho formation[J]. *Tunnelling and Underground Space Technology*, 2000, 15(1): 49-54.
- [19] Lu GM, Li YH, Hassani F, Zhang XW. Review of theoretical and experimental studies on mechanical rock fragmentation using microwave-assisted approach[J]. *Chinese Journal of Geotechnical Engineering*, 2016, 38(8): 1497-1506.
- [20] Zheng YL, Ma ZJ, Zhao XB, He L. Experimental investigation on the thermal, mechanical and cracking behaviours of three Igneous rocks under microwave treatment[J]. *Rock Mechanics and Rock Engineering*, 2020.
- [21] Zheng YL, Zhang QB, Zhao J. Effect of microwave treatment on thermal and ultrasonic properties of gabbro[J]. *Applied Thermal Engineering*, 2017, 127: 359-369.
- [22] Li X, Wang S, Xu Y, Yao W, Xia K, Lu G. Effect of microwave irradiation on dynamic mode-I fracture parameters of Barre granite[J]. *Engineering Fracture Mechanics*, 2019, 224: 106748.
- [23] Toifl M, Hartlieb P, Meisels R, Antretter T, Kuchar F. Numerical study of the influence of irradiation parameters on the microwave-induced stresses in granite[J]. *Minerals Engineering*, 2017, 103-104(4): 78-92.
- [24] Ali AY, Bradshaw SM. Confined particle bed breakage of microwave treated and untreated ores[J]. *Minerals Engineering*, 2011, 24(14): 1625-1630.
- [25] Jones DA, Kingman SW, Whittles DN, Lowndes IS. The influence of microwave energy delivery method on strength reduction in ore samples[J]. *Chemical Engineering and Processing: Process Intensification*, 2007, 46(4): 291-299.
- [26] Kingman SW, Corfield GM, Rowson NA. Effects of microwave radiation upon the mineralogy and magnetic processing of a massive Norwegian ilmenite ore[J]. *Magnetic and Electrical Separation*, 1998, 9(3): 131-148.
- [27] Kingman SW, Vorster W, Rowson NA. The influence of mineralogy on microwave assisted grinding[J]. *Minerals Engineering*, 2000, 13(3): 313-327.
- [28] Vorster W, Rowson NA, Kingman SW. The effect of microwave radiation upon the processing of Neves Corvo copper ore[J]. *International Journal of Mineral Processing*, 2001, 63(1): 29-44.
- [29] Lu GM, Feng XT, Li YH, Hassani F, Zhang X. Experimental investigation on the effects of microwave treatment on basalt heating, mechanical strength, and fragmentation[J]. *Rock Mechanics and Rock Engineering*, 2019, 52(8): 2535-2549.
- [30] Kingman SW, Jackson K, Bradshaw SM, Rowson NA, Greenwood R. An investigation into the influence of microwave treatment on mineral ore comminution[J]. *Powder Technology*, 2004, 146(3): 176-184.
- [31] Li Yuan-hui, Lu Gao-ming, Feng Xia-ting, Zhang Xiwei. The influence of heating path on the effect of hard rock fragmentation using microwave assisted method[J]. *Chinese Journal of Rock Mechanics and Engineering*, 2017, 36(6): 1460-1468.
- [32] Hassani F, Nekoovaght PM, Radziszewski P, Waters KE. Microwave assisted mechanical rock breaking[C]// *Proceedings of the 12th ISRM*

International Congress on Rock Mechanics, Beijing: International Society for Rock Mechanics, 2011: 2075-2080.

[33] Nekoovaght P, Hassani F. The influence of microwave radiation on hard rocks as in microwave assisted rock breakage applications[M]. Boca Raton: Rock Engineering and Rock Mechanics: Structures in and on Rock Masses, 2014: 195-198.

[34] Nekoovaght P, Gharib N, Hassani F. Numerical simulation and experimental investigation of the influence of 2.45 GHz microwave radiation on hard rock surface[C]// ISRM International Symposium—8th Asian Rock Mechanics, Sapporo, Japan: International Society for Rock Mechanics, 2014.

[35] Peinsitt T, Kuchar F, Hartlieb P, Moser P, Kargl H, Restner U, Sifferlinger N. Microwave heating of dry and water saturated basalt, granite and sandstone[J]. International Journal of Mining and Mineral Engineering, 2010, 2(1): 18-29.

[36] Hartlieb P, Kuchar F, Moser P, Kargl H, Restner U. Reaction of different rock types to low-power (3.2 kW) microwave irradiation in a multimode cavity[J]. Minerals Engineering, 2018, 118: 37-51.

[37] Hartlieb P, Toifl M, Kuchar F, Meisels R, Antretter T. Thermo-physical properties of selected hard rocks and their relation to microwave-assisted comminution[J]. Minerals Engineering, 2016, 91: 34-41.

[38] Hartlieb P, Leindl M, Kuchar F, Antretter T, Moser P. Damage of basalt induced by microwave irradiation[J]. Minerals Engineering, 2012, 31(3): 82-89.

[39] Lu GM, Zhou JJ, Li YH, Zhang X, Gao WY. The influence of minerals on

the mechanism of microwave-induced fracturing of rocks[J]. Journal of Applied Geophysics, 2020, 180: 1-11.

[40] Lu GM, Li YH, Hassani F, Zhang X. The influence of microwave irradiation on thermal properties of main rock-forming minerals[J]. Applied Thermal Engineering, 2017, 112(2): 1523-1532.

[41] Chantrey P. Industrial Microwave Heating[M]. London: Peter Peregrinus Ltd, 1983: 1-659.

[42] Meredith R. Engineers' handbook of industrial microwave heating[J]. Engineers' handbook of industrial microwave heating [Book Review], 1998, 13(1): 3-3.

[43] Ahrens TJ. Mineral physics and crystallography: a handbook of physical constants[M]. Washington, dc: American Geophysical Union, 1995.

[44] Lu GM, Sun ZC, Zhou JJ, Chen K, Li FY. Effect of Microwave irradiation on computed tomography and acoustic emission characteristics of hard rock[J]. Geotechnical and Geological Engineering, 2020.

[45] Lu GM, Feng XT, Li YH, Zhang X. Influence of microwave treatment on mechanical behaviour of compact basalts under different confining pressures[J]. Journal of Rock Mechanics and Geotechnical Engineering, 2020, 12(2): 1-10.